

Heterogeneous Power-Splitting Based Two-Way DF Relaying with Non-Linear Energy Harvesting

Liqin Shi¹, Wenchi Cheng¹, Yinghui Ye¹, Hailin Zhang¹, and Rose Qingyang Hu²

¹State Key Laboratory of Integrated Services Networks, Xidian University, China

²Department of Electrical and Computer Engineering, Utah State University, USA

Abstract—Simultaneous wireless information and power transfer (SWIPT) has been recognized as a promising approach to improving the performance of energy constrained networks. In this paper, we investigate a SWIPT based three-step two-way decode-and-forward (DF) relay network with a non-linear energy harvester equipped at the relay. As most existing works require instantaneous channel state information (CSI) while CSI is not fully utilized when designing power splitting (PS) schemes, there exists an opportunity for enhancement by exploiting CSI for PS design. To this end, we propose a novel heterogeneous PS scheme, where the PS ratios are dynamically changed according to instantaneous channel gains. In particular, we derive the closed-form expressions of the optimal PS ratios to maximize the capacity of the investigated network and analyze the outage probability with the optimal dynamic PS ratios based on the non-linear energy harvesting (EH) model. The results provide valuable insights into the effect of various system parameters, such as transmit power of the source, source transmission rate, and source to relay distance on the performance of the investigated network. The results show that our proposed PS scheme outperforms the existing schemes.

Index Terms—Simultaneous wireless information and power transfer, two-way decode-and-forward relay, dynamic heterogeneous power splitting, non-linear energy harvesting.

I. INTRODUCTION

Recently, simultaneous wireless information and power transfer (SWIPT) has emerged as an appealing approach to prolonging the lifetime of energy-constrained networks, e.g., relay networks [1], [2], wireless sensor networks [3], cooperative non-orthogonal multiple access networks [4], D2D assisted cellular networks [5], by harvesting energy from radio frequency (RF) signals. Of particular interest is integrating SWIPT with relay networks, which not only extends the wireless transmission range, but also prolongs the operating time of the energy-constrained relay nodes [4], [6]. Compared with one-way relaying, two-way relaying, which can be performed in two steps or three steps, can offer a more efficient use of the available resources by allowing two destination nodes to exchange information with each other. Regarding this consideration, increasing attention has been paid to the SWIPT based two-way relay networks (TWRNs), where wireless signals are either switched in the time domain or split in the power domain to facilitate SWIPT, i.e., time switching (TS) scheme and power splitting (PS) scheme.

Some studies on the design of TS/PS scheme for two-step TWRNs [7], [8] have been hitherto reported. The authors of [7] studied the optimal TS/PS scheme for amplify-and-forward (AF) and decode-and-forward (DF) based TWRNs. It was

shown that at high signal-to-noise (SNR) ratio, the PS scheme can achieve a larger sum rate than the TS scheme. The authors of [8] proposed a resource allocation strategy, which jointly optimizes the time allocation ratio and the PS/TS ratio, to minimize the outage probability of DF based TWRNs.

Since the low complexity of hardware is very vital to energy-constrained networks, three-step two-way relaying has attracted extensive research interests [9]–[12]. Based on the TS receiver, three wireless power transfer policies have been proposed to maximize the capacity [9]. A static equal PS scheme has been developed to maximize the overall outage capacity for three-step AF TWRNs [10], where the PS ratio is determined by the statistical channel state information (CSI). The outage capacity can be improved by adopting a dynamic PS scheme, because the PS ratio can be adaptive to the instantaneous CSI instead of to the statistical CSI. For this reason, the dynamic equal PS scheme was further developed [11]. Recently, the three-step AF relay has also been extended to the DF relay system [12], where the upper and lower bounds of the outage probability with respect to the static equal PS scheme were studied. Note that although the instantaneous CSI is required at both destinations to perform successive interference cancellation (SIC) [12], it is not used in determining the PS ratio. Moreover, as the channel gains between the source nodes and the relay are both heterogeneous and instantaneously changing, a PS scheme based on both heterogeneous and instantaneous CSI can achieve more efficient transmission than the equal PS scheme.

Motivated by the reasons stated above, we propose a dynamic heterogeneous PS scheme, where the PS ratio for each link can be dynamically adjusted based on its instantaneous CSI, and apply it into the SWIPT based three-step DF TWRNs. Unlike the works mentioned above [9]–[12], we consider a non-linear energy harvesting (EH) model [13] instead of the conventional linear one and study the outage capacity of the proposed scheme in the investigated network.

The main contributions of this paper are summarized as follows.

- We propose a novel dynamic heterogeneous PS scheme to maximize the capacity of SWIPT based DF TWRNs with the non-linear EH model and derive the closed-form expressions for the optimal PS ratios. Compared with the scheme in [12], the proposed scheme is more flexible and can achieve better performance.
- We analyze the outage capacity with the optimal PS ratios, as an effort to know how much performance gain the

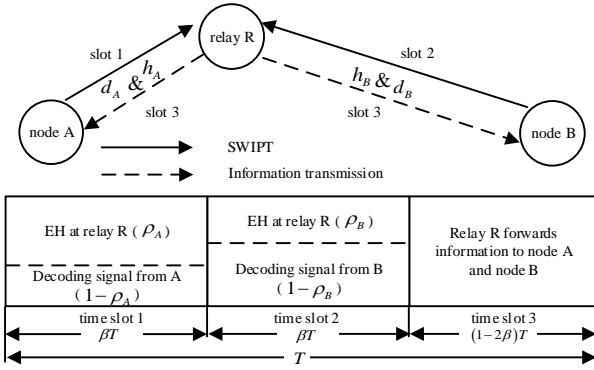


Fig. 1. System model of the three-step two-way DF relay network.

designed scheme could offer in the investigated network. Simulation results verify the correctness of the derived results and demonstrate that the proposed PS scheme can significantly improve the capacity of the investigated system as compared with the existing schemes.

The remainder of this paper is organized as follows. The system model is provided in Section II. In Section III, we propose a novel dynamic heterogeneous PS scheme to maximize the capacity of SWIPT based DF TWRNs with the non-linear EH model and analyze the corresponding outage performance. Simulation results are provided in Section IV, followed by conclusions in Section V.

II. SYSTEM MODEL

As shown in Fig. 1, we consider a three-step two-way DF relay network, where two destination nodes A and B exchange information via an energy-constrained relay node R . Each node is equipped with a single antenna and works in the half-duplex mode. There is no direct link between A and B due to severe path loss and shadowing. The path loss model is given by $|h_i|^2 d_i^{-\alpha}$ ($i = A$ or B), where h_i is the i - R channel coefficient, d_i is the i - R distance, and α is the path loss exponent. All the channels are assumed to undergo independent identically distributed (i.i.d) quasi-static Rayleigh fading and all the channels are assumed to be reciprocal. Note that the use of such channels can be found widely in prior research in this field [5], [12], [14]. Let T denote the total transmission block which can be divided into three time slots. Let $\beta \in (0, 0.5)$ be the time proportion for R to harvest energy and decode signals from A or B . The transmission time for A or B to R is βT . After receiving signal from i ($i = A$ or B), R splits it into two parts with ratio ρ_i with one part used for energy harvesting and the other part used for information processing. In the remaining block time $(1-2\beta)T$, R decodes the signals and forwards them to A and B .

At the first or the second time slot with βT , A or B transmits the signal s_A or s_B to R and the received RF signal from i ($i = A$ or B) at R is given by

$$y_{iR} = h_i \sqrt{P_i d_i^{-\alpha}} s_i + n_{iR}, \quad (1)$$

where P_i denotes the transmit power of i , $\mathbb{E}\{|s_i|^2\} = 1$ and $n_{iR} \sim \mathcal{CN}(0, \sigma_{iR}^2)$ is the additive white Gaussian noise (AWGN).

Thus, the received power from i at R before the third time slot is given by

$$P_{\text{RF}}^i = \rho_i P_i |h_i|^2 d_i^{-\alpha}. \quad (2)$$

Since the conventional linear EH model cannot capture the practical EH circuit due to the nonlinearity of the diodes, inductors and capacitors [15], we employ a more practical non-linear EH model in [13], which has been verified by comparing with measurement data from [16] and [17]. Compared with the non-linear EH model in [15], the model in [13], namely piecewise linear EH model, is more mathematically tractable, and able to provide sufficient precision by selecting the proper number of segments (see Fig. 2 in [13]). According to the piecewise linear EH model in [13], the harvested power P_{H}^i from i can be modelled as

$$P_{\text{H}}^i = \begin{cases} 0, & P_{\text{RF}}^i < P_{\text{th}}^1; \\ a_j P_{\text{RF}}^i + b_j, & P_{\text{RF}}^i \in [P_{\text{th}}^j, P_{\text{th}}^{j+1}], j = 1, \dots, N-1; \\ P_{\text{m}}, & P_{\text{RF}}^i > P_{\text{th}}^N, \end{cases} \quad (3)$$

where $P_{\text{th}} = \{P_{\text{th}}^j | 1 \leq j \leq N\}$ are the thresholds on P_{RF}^i for $N+1$ linear segments¹, a_j and b_j are the slope and the intercept for the linear function in the j -th segment, respectively, and P_{m} denotes the maximum harvestable power when the circuit is saturated.

Then, the total harvested energy is²

$$E_{\text{total}} = \beta T (P_{\text{H}}^i + P_{\text{H}}^{\bar{i}}) \\ = \beta T (a_j \rho_i P_i |h_i|^2 d_i^{-\alpha} + a_k \rho_{\bar{i}} P_{\bar{i}} |h_{\bar{i}}|^2 d_{\bar{i}}^{-\alpha} + b_k + b_j), \quad (4)$$

where $j, k \in \{0, \dots, N\}$ denote to which segment P_{RF}^i or $P_{\text{RF}}^{\bar{i}}$ belongs. Let the segment with $P_{\text{RF}}^i < P_{\text{th}}^1$ be the 0-th segment and the segment with $P_{\text{RF}}^i > P_{\text{th}}^N$ be the N -th segment. Based on Eq. (3), we have $a_0 = b_0 = a_N = 0$, $b_N = P_{\text{m}}$. According to [13], both $\{a_j\}_1^{N-1}$ and $\{b_j\}_1^{N-1}$ are obtained by linear regression to minimize the difference with the practical EH circuit. Thus, a_j and b_j in j -th ($j = 1, \dots, N-1$) segment are given by

$$\begin{cases} a_j = \frac{\sum_{l=1}^n (x_l - \bar{x})(y_l - \bar{y})}{\sum_{l=1}^n (x_l - \bar{x})^2} = \frac{\sum_{l=1}^n x_l y_l - n \bar{x} \bar{y}}{\sum_{l=1}^n x_l^2 - n \bar{x}^2}; \\ b_j = \bar{y} - a_j \bar{x}, \end{cases} \quad (5)$$

where $\{(x_1, y_1), (x_2, y_2), \dots, (x_{n-1}, y_{n-1}), (x_n, y_n)\}$ denote the experimental data in the j -th segment, $\bar{x} = \frac{\sum_{l=1}^n x_l}{n}$, and $\bar{y} = \frac{\sum_{l=1}^n y_l}{n}$.

For the information processing, the received SNR for decoding s_i is

$$\gamma_{iR} = \frac{P_i |h_i|^2 (1 - \rho_i)}{d_i^\alpha \sigma_i^2}. \quad (6)$$

¹Note that the P_{th}^1 represents the power sensitivity for the EH circuits.

²If $i = A$, $\bar{i} = B$; if $i = B$, $\bar{i} = A$.

Let \tilde{s}_A and \tilde{s}_B denote the decoded signals for A and B during the first and the second time slots, respectively. In the third time slot, R combines \tilde{s}_A and \tilde{s}_B and broadcasts the normalized signal $s_R = \frac{\tilde{s}_A + \tilde{s}_B}{\sqrt{2}}$ to both A and B with the harvested energy E_{total} . Then the received signal at i is given by

$$\begin{aligned} y_{Ri} &= h_i \sqrt{P_R d_i^{-\alpha}} s_R + n_{Ri} \\ &\stackrel{(a)}{=} h_i \sqrt{P_R d_i^{-\alpha}} \frac{\tilde{s}_i}{\sqrt{2}} + \tilde{n}_{Ri}, \end{aligned} \quad (7)$$

where $P_R = \frac{E_{\text{total}}}{(1-2\beta)T}$ is the transmit power at R , $n_{Ri} = \tilde{n}_{Ri} \sim \mathcal{CN}(0, \sigma_{Ri}^2)$ is the AWGN caused by the receiving antenna at i , (a) follows by using SIC due to the fact that the CSI and other system parameters are available at i , and \tilde{i} denotes the index of the other destination node.

For analytical simplicity, we assume $P_A = P_B = P$ and $\sigma_{AR}^2 = \sigma_{BR}^2 = \sigma_{RA}^2 = \sigma_{RB}^2 = \sigma^2$. Based on Eq. (7), the end-to-end SNR of the link $\tilde{i} \xrightarrow{R} i$ is given by

$$\begin{aligned} \gamma_{Ri} &= \frac{P_R |h_i|^2}{2d_i^\alpha \sigma^2} = a_j \rho_i P |h_i|^4 X d_i^{-2\alpha} \\ &\quad + X d_i^{-\alpha} (a_k \rho_i P |h_i|^2 |h_i|^2 d_i^{-\alpha} + (b_k + b_j) |h_i|^2), \end{aligned} \quad (8)$$

where $X = \frac{\beta}{2(1-2\beta)\sigma^2}$.

III. PERFORMANCE ANALYSIS

In this section, we first derive the closed-form expression for the optimal dynamic heterogeneous PS ratios, ρ_A^* and ρ_B^* , respectively, to maximize the capacity of the system. Then, an analytical expression of the outage probability with ρ_A^* and ρ_B^* under the piecewise linear EH model is provided.

A. Dynamic Heterogeneous PS Scheme

Let $\mathbb{P}(\cdot)$ denote the probability. Let P_{out}^i be the outage probability at node i . For a predefined threshold γ_{th} , P_{out}^i is given by

$$P_{\text{out}}^i = \underbrace{\mathbb{P}(\gamma_{iR} < \gamma_{\text{th}})}_{P_1} + \underbrace{\mathbb{P}(\gamma_{Ri} < \gamma_{\text{th}}, \gamma_{iR} \geq \gamma_{\text{th}})}_{P_2}, \quad (9)$$

where P_1 is the outage probability at the relay and P_2 is the outage probability at the destination node i .

According to [12], [18], the capacity of the system can be calculated as

$$C_{\text{total}} = (2 - P_{\text{out}}^A - P_{\text{out}}^B) UT \times \min(\beta, 1 - 2\beta) \quad (10)$$

where $U = \log_2(1 + \gamma_{\text{th}})$ is the source transmission rate of nodes A , B , and R . Then we formulate the optimization problem to maximize the capacity of the system as

$$\begin{aligned} P1 : & \text{maximize } C_{\text{total}} \\ & \text{subject to } (\rho_A, \rho_B) \\ & \text{s.t. } : 0 \leq \rho_i < 1, i \in \{A, B\}. \end{aligned} \quad (11)$$

Based on Eq. (9), the optimization problem can be transformed into

$$\begin{aligned} P2 : & \text{maximize } \mathbb{P}(\gamma_{RA} \geq \gamma_{\text{th}}) + \mathbb{P}(\gamma_{RB} \geq \gamma_{\text{th}}) \\ & \text{subject to } (\rho_A, \rho_B) \\ & \text{s.t. } : 0 \leq \rho_i \leq \max\left\{1 - \frac{\gamma_{\text{th}} d_i^\alpha \sigma^2}{P |h_i|^2}, 0\right\}, i \in \{A, B\}. \end{aligned} \quad (12)$$

Note that $P_1 = 1$ always holds when $1 - \frac{\gamma_{\text{th}} d_i^\alpha \sigma^2}{P |h_i|^2} < 0$. Since both γ_{RA} and γ_{RB} increase with the increasing of ρ_i with a given $\rho_{\tilde{i}}$, it is readily seen that the optimal solution to P_2 can be obtained when $\rho_A = \max\left\{1 - \frac{\gamma_{\text{th}} d_A^\alpha \sigma^2}{P |h_A|^2}, 0\right\}$ and $\rho_B = \max\left\{1 - \frac{\gamma_{\text{th}} d_B^\alpha \sigma^2}{P |h_B|^2}, 0\right\}$. Thus, the optimal dynamic PS ratio ρ_i^* is given by

$$\rho_i^* = \max\left\{1 - \frac{\gamma_{\text{th}} d_i^\alpha \sigma^2}{P |h_i|^2}, 0\right\}. \quad (13)$$

B. End-to-End Outage Probability with ρ_i^*

Based on Eq. (9), P_{out}^B can be expressed as

$$P_{\text{out}}^B = \underbrace{\mathbb{P}(\gamma_{AR} < \gamma_{\text{th}})}_{P_{31}} + \underbrace{\mathbb{P}(\gamma_{RB} < \gamma_{\text{th}}, \gamma_{AR} \geq \gamma_{\text{th}})}_{P_{32}}, \quad (14)$$

where P_{31} is the outage probability at relay R and P_{32} is the outage probability at destination B . Substituting the optimal PS ratios in Eq. (13) into Eq. (14), we have

$$P_{31} = \mathbb{P}\left(|h_A|^2 < \frac{\gamma_{\text{th}} d_A^\alpha \sigma^2}{P}\right) \stackrel{(b)}{=} 1 - \exp\left(-\frac{\varpi d_A^\alpha}{\lambda_A}\right), \quad (15)$$

where (b) holds due to $|h_A|^2 \sim \exp\left(\frac{1}{\lambda_A}\right)$ and $\varpi = \frac{\gamma_{\text{th}} \sigma^2}{P}$.

There are two cases for the value of ρ_B^* , which are 0 for the case with $1 - \frac{\gamma_{\text{th}} d_B^\alpha \sigma^2}{P |h_B|^2} < 0$ and $1 - \frac{\gamma_{\text{th}} d_B^\alpha \sigma^2}{P |h_B|^2}$ for the other case. Combining with the piecewise linear EH model in Eq. (3), there are $N + 1$ pairs for values of (a_j, b_j) . Thus, P_{32} is given by

$$P_{32} = \underbrace{\sum_{k=0}^N P_{321}^k}_{P_{21}} + \underbrace{\sum_{j=0}^N \sum_{k=0}^N P_{322}^{j,k}}_{P_{22}}, \quad (16)$$

where P_{321}^k is the part of P_{32} where the energy harvester operates in the k -th linear region for P_{RF}^A with $\rho_B^* = 0$ and $P_{322}^{j,k}$ is the part of P_{32} where the energy harvester operates in the k -th linear region for P_{RF}^A and the j -th linear region for P_{RF}^B with $\rho_B^* = 1 - \frac{\gamma_{\text{th}} d_B^\alpha \sigma^2}{P |h_B|^2}$.

Based on the above two cases, if $|h_B|^2 < \varpi d_B^\alpha$ is satisfied, we have P_{321}^k as

$$P_{321}^k = \mathbb{P}\left(a_k |h_A|^2 < \frac{Y^{A1}}{|h_B|^2} + Y_{0,k}^{A3}, |h_A|^2 \geq \varpi d_A^\alpha, |h_B|^2 < \varpi d_B^\alpha\right), \quad (17)$$

where $Y^{A1} = \frac{\gamma_{\text{th}} d_B^\alpha d_A^\alpha}{P X}$ and $Y_{j,k}^{A3} = [\varpi (a_k + a_j) - \frac{b_k + b_j}{P}] d_A^\alpha$. If $|h_B|^2 \geq \varpi d_B^\alpha$, $P_{322}^{j,k}$ are

$$P_{322}^{j,k} = \mathbb{P}\left(a_k \varpi d_A^\alpha \leq a_k |h_A|^2 < \frac{Y^{A1}}{|h_B|^2} + Y_j^{A2} |h_B|^2 + Y_{j,k}^{A3}, |h_B|^2 \geq \varpi d_B^\alpha\right), \quad (18)$$

where $Y_j^{A2} = -\frac{a_j d_A^\alpha}{d_B^\alpha}$.

1) *The derivation of P_{21}* : Based on the value of k and the piecewise linear EH model in Eq. (3), there are three cases for P_{321}^k as follows.

Case I: When $k = 0$, we have $a_k = b_k = 0$ and $P_{\text{RF}}^A < P_{\text{th}}^1$. Combining with $|h_B|^2 < \varpi d_B^\alpha$ is given by

$$P_{321}^0 = \mathbb{P}\left(0 < Y^{A1}, \varpi d_A^\alpha \leq |h_A|^2 < (\varpi + \theta_1)d_A^\alpha, |h_B|^2 < \varpi d_B^\alpha\right) \\ \stackrel{(c)}{=} \left[1 - \exp\left(-\frac{\varpi d_B^\alpha}{\lambda_B}\right)\right] \left[\exp\left(-\frac{\varpi d_A^\alpha}{\lambda_A}\right) - \exp\left(-\frac{(\theta_1 + \varpi)d_A^\alpha}{\lambda_A}\right)\right], \quad (19)$$

where (c) holds due to $|h_B|^2 \sim \exp\left(\frac{1}{\lambda_B}\right)$ and $\theta_1 = \frac{P_{\text{th}}^1}{P}$.

Case II: When $k = N$, we have $a_k = 0, b_k = P_m$. Let $\theta_k = \frac{P_{\text{th}}^k}{P}$. Then $|h_A|^2 > (\varpi + \theta_N)d_A^\alpha$ and P_{321}^N is given by

$$P_{321}^N = \mathbb{P}\left(0 < \frac{Y^{A1}}{|h_B|^2} + Y_{0,N}^{A3}, |h_A|^2 > (\varpi + \theta_N)d_A^\alpha, |h_B|^2 < \varpi d_B^\alpha\right) \\ = \exp\left(-\frac{(\varpi + \theta_N)d_A^\alpha}{\lambda_A}\right) \left[1 - \exp\left(-\frac{\delta^0}{\lambda_B}\right)\right], \quad (20)$$

where $\delta^0 = \min\left(\frac{\gamma_{\text{th}} d_B^\alpha}{P_m X}, \varpi d_B^\alpha\right)$.

Case III: When $k \in \{1, \dots, N-1\}$, we have $a_k \neq 0$ and $(\varpi + \theta_k)d_A^\alpha \leq |h_A|^2 \leq (\varpi + \theta_{k+1})d_A^\alpha$. Based on Eq. (17), P_{321}^k is given by

$$P_{321}^k = \mathbb{P}\left(|h_B|^2 < \varpi d_B^\alpha, (\varpi + \theta_k)d_A^\alpha \leq |h_A|^2 \leq \phi_{\text{max}}^k(|h_B|^2)\right) \\ \stackrel{(d)}{=} \int_0^{\varpi d_B^\alpha} \int_{(\varpi + \theta_k)d_A^\alpha}^{\phi_{\text{max}}^k(x)} \frac{1}{\lambda_B} \exp\left(-\frac{x}{\lambda_B}\right) \frac{1}{\lambda_A} \exp\left(-\frac{y}{\lambda_A}\right) dy dx \\ = \exp\left[-\frac{(\varpi + \theta_k)d_A^\alpha}{\lambda_A}\right] - \exp\left[-\frac{(\varpi + \theta_k)d_A^\alpha}{\lambda_A}\right] \exp\left(-\frac{\delta_{\text{max}}^k}{\lambda_B}\right) \\ - \exp\left[-\frac{(\varpi + \theta_{k+1})d_A^\alpha}{\lambda_A}\right] \left[1 - \exp\left(-\frac{\delta_{\text{min}}^k}{\lambda_B}\right)\right] \\ - \frac{\exp\left(-\frac{\varpi d_A^\alpha}{\lambda_A}\right)}{\lambda_B} \underbrace{\int_{\delta_{\text{min}}^k}^{\delta_{\text{max}}^k} \exp\left(-\frac{Y^{A1}}{a_k \lambda_A x} - \frac{x}{\lambda_B}\right) dx}_{\Xi}, \quad (21)$$

where (d) holds from $y = |h_A|^2$ and $x = |h_B|^2$ and

$$\begin{cases} \phi_{\text{max}}^k(x) = \\ \max\left[\min\left((\varpi + \theta_{k+1})d_A^\alpha, \frac{Y^{A1}}{a_k \theta_{k+1}} + \varpi d_A^\alpha\right), (\varpi + \theta_k)d_A^\alpha\right], \\ \delta_{\text{min}}^k = \min\left[\max\left(\frac{Y^{A1}}{d_A^\alpha a_k \theta_{k+1}}, 0\right), \varpi d_B^\alpha\right], \\ \delta_{\text{max}}^k = \max\left[\min\left(\frac{Y^{A1}}{d_A^\alpha a_k \theta_k}, \varpi d_B^\alpha\right), \delta_{\text{min}}^k\right]. \end{cases}$$

Note that it is difficult to find the accurate closed-form expression for P_{321}^k with $Y_{0,k}^{A1} > 0$ due to the integral $\int_{s_1}^{s_2} \exp(z_1 x + \frac{z_2}{x}) dx$ with any value of z_1 and $z_2 \neq 0$. Fortunately, we can use Gaussian-Chebyshev quadrature to find an approximation for P_{321}^k . According to [14], Gaussian-Chebyshev quadrature is defined as $\int_{t_1}^{t_2} f(\xi) d\xi \approx \frac{t_2 - t_1}{2} \sum_{j=1}^K w_j \sqrt{1 - z_j^2} f(\xi_j)$, where $w_j = \frac{\pi}{K}$, $z_j = \cos \frac{2j-1}{2K} \pi$ and $\xi_j = \frac{t_2 - t_1}{2} z_j + \frac{t_2 + t_1}{2}$. Thus, Ξ can be calculated as

$$\Xi \approx \frac{\pi(\delta_{\text{max}}^k - \delta_{\text{min}}^k)}{2M} \sum_{m=1}^M \sqrt{1 - \nu_m^2} \exp\left(-\frac{Y^{A1}}{a_k \lambda_A \kappa_m^k} - \frac{\kappa_m^k}{\lambda_B}\right), \quad (22)$$

where M is a parameter that determines the tradeoff between complexity and accuracy, $\nu_m = \cos \frac{2m-1}{2M} \pi$, and $\kappa_m^k =$

$\frac{(\delta_{\text{max}}^k - \delta_{\text{min}}^k)}{2} \nu_m + \frac{(\delta_{\text{max}}^k + \delta_{\text{min}}^k)}{2}$. Note that a larger M results in a higher accuracy while a moderate yet acceptable accuracy can be realized at a small M . This is verified in our simulation results. Based on Eqs. (19), (20), and (21), the approximation of P_{21} can be obtained.

2) *The derivation of P_{22}* : Likewise, we derive the expression of P_{22} as follows. Given the values of j and k , $P_{322}^{j,k}$ is expressed as follows.

Case 1: When $j = 0$ with $\rho_B^* = 1 - \frac{\gamma_{\text{th}} d_B^\alpha \sigma^2}{P|h_B|^2}$, we have $a_j = b_j = 0$ and $\varpi d_B^\alpha \leq |h_B|^2 < (\theta_1 + \varpi)d_B^\alpha$. Based on Eq. (18), the expression of $P_{322}^{0,k}$ is given by

$$P_{322}^{0,k} = \mathbb{P}\left(a_k |h_A|^2 < \frac{Y^{A1}}{|h_B|^2} + Y_{0,k}^{A3} |h_A|^2 \geq \varpi d_A^\alpha, \varpi d_B^\alpha \leq |h_B|^2 < (\theta_1 + \varpi)d_B^\alpha\right). \quad (23)$$

Similarly, when $k = 0$, we have

$$P_{322}^{0,0} = \left[\exp\left(-\frac{\varpi d_B^\alpha}{\lambda_B}\right) - \exp\left(-\frac{(\theta_1 + \varpi)d_B^\alpha}{\lambda_B}\right)\right] \\ \times \left[\exp\left(-\frac{\varpi d_A^\alpha}{\lambda_A}\right) - \exp\left(-\frac{(\theta_1 + \varpi)d_A^\alpha}{\lambda_A}\right)\right].$$

When $k \in \{1, \dots, N-1\}$, $P_{322}^{0,k}$ can be calculated as

$$P_{322}^{0,k} \approx \exp\left(-\frac{(\varpi + \theta_k)d_A^\alpha}{\lambda_A} - \frac{\varpi d_B^\alpha}{\lambda_B}\right) - \exp\left(-\frac{(\varpi + \theta_k)d_A^\alpha}{\lambda_A} - \frac{\delta_{\text{max}}^{0,k}}{\lambda_B}\right) \\ - \exp\left(-\frac{(\varpi + \theta_{k+1})d_A^\alpha}{\lambda_A}\right) \left[\exp\left(-\frac{\varpi d_B^\alpha}{\lambda_B}\right) - \exp\left(-\frac{\delta_{\text{min}}^{0,k}}{\lambda_B}\right)\right] \\ - \exp\left(-\frac{\varpi d_A^\alpha}{\lambda_A}\right) \frac{\pi(\delta_{\text{max}}^{0,k} - \delta_{\text{min}}^{0,k})}{2M\lambda_B} \\ \times \sum_{m=1}^M \sqrt{1 - \nu_m^2} \exp\left(-\frac{Y^{A1}}{a_k \lambda_A \kappa_m^{0,k}} - \frac{\kappa_m^{0,k}}{\lambda_B}\right), \quad (24)$$

where

$$\begin{cases} \delta_{\text{min}}^{0,k} = \min\left[\max\left(\frac{Y^{A1}}{d_A^\alpha a_k \theta_{k+1}}, \varpi d_B^\alpha\right), (\theta_1 + \varpi)d_B^\alpha\right], \\ \delta_{\text{max}}^{0,k} = \max\left[\min\left(\frac{Y^{A1}}{d_A^\alpha a_k \theta_k}, (\theta_1 + \varpi)d_B^\alpha\right), \delta_{\text{min}}^{0,k}\right], \\ \kappa_m^{0,k} = \frac{(\delta_{\text{max}}^{0,k} - \delta_{\text{min}}^{0,k})}{2} \nu_m + \frac{(\delta_{\text{max}}^{0,k} + \delta_{\text{min}}^{0,k})}{2}. \end{cases}$$

When $k = N$, $P_{322}^{0,N}$ is given by

$$P_{322}^{0,N} = \exp\left(-\frac{(\varpi + \theta_N)d_A^\alpha}{\lambda_A}\right) \left[\exp\left(-\frac{\varpi d_B^\alpha}{\lambda_B}\right) - \exp\left(-\frac{\delta^{0,N}}{\lambda_B}\right)\right], \quad (25)$$

where $\delta^{0,N} = \max\left(\min\left[\frac{\gamma_{\text{th}} d_B^\alpha}{P_m X}, (\theta_1 + \varpi)d_B^\alpha\right], \varpi d_B^\alpha\right)$.

Case 2: When $j = N$, we have $a_j = 0$ and $b_j = P_m$. Thus, $P_{322}^{N,k}$ is given by $\mathbb{P}\left(a_k |h_A|^2 < \frac{Y^{A1}}{|h_B|^2} + Y_{N,k}^{A3} |h_A|^2 \geq \varpi d_A^\alpha, |h_B|^2 > (\varpi + \theta_N)d_B^\alpha\right)$.

Similar to the derivation of P_{21} , if $k = 0$, $P_{322}^{N,0}$ can be calculated as

$$P_{322}^{N,0} = \left[\exp\left(-\frac{(\varpi + \theta_N)d_B^\alpha}{\lambda_B}\right) - \exp\left(-\frac{\delta^{N,0}}{\lambda_B}\right)\right] \\ \times \left[\exp\left(-\frac{\varpi d_A^\alpha}{\lambda_A}\right) - \exp\left(-\frac{(\theta_1 + \varpi)d_A^\alpha}{\lambda_A}\right)\right], \quad (26)$$

where $\delta^{N,0} = \max\left[\frac{\gamma_{\text{th}} d_B^\alpha}{P_m X}, (\theta_N + \varpi)d_B^\alpha\right]$.

If $k \in \{1, \dots, N-1\}$, $P_{322}^{N,k}$ can be computed as

$$\begin{aligned}
P_{322}^{N,k} &\approx \exp\left(-\frac{(\varpi+\theta_k)d_A^\alpha}{\lambda_A} - \frac{(\varpi+\theta_N)d_B^\alpha}{\lambda_B}\right) - \exp\left(-\frac{(\varpi+\theta_k)d_A^\alpha}{\lambda_A} - \frac{\delta_{\max}^{N,k}}{\lambda_B}\right) \\
&\quad - \left[\exp\left(-\frac{(\varpi+\theta_N)d_B^\alpha}{\lambda_B}\right) - \exp\left(-\frac{\delta_{\min}^{N,k}}{\lambda_B}\right) \right] \times \\
&\quad \exp\left(-\frac{(\varpi+\theta_{k+1})d_A^\alpha}{\lambda_A}\right) - \exp\left(-\frac{\varpi d_A^\alpha}{\lambda_A}\right) \frac{\pi(\delta_{\max}^{N,k} - \delta_{\min}^{N,k})}{2M\lambda_B} \\
&\quad \times \sum_{m=1}^M \sqrt{1 - \nu_m^2} \exp\left(-\frac{Y^{A1}}{a_k \lambda_A \kappa_m^{N,k}} - \frac{\kappa_m^{N,k}}{\lambda_B}\right), \quad (27)
\end{aligned}$$

where

$$\begin{cases} \delta_{\min}^{N,k} = \max\left(\frac{Y^{A1}}{d_A^\alpha a_k \theta_{k+1}}, (\varpi + \theta_N)d_B^\alpha\right), \\ \delta_{\max}^{N,k} = \max\left(\frac{Y^{A1}}{d_A^\alpha a_k \theta_k}, (\varpi + \theta_N)d_B^\alpha\right), \\ \kappa_m^{N,k} = \frac{(\delta_{\max}^{N,k} - \delta_{\min}^{N,k})}{2} \nu_m + \frac{(\delta_{\max}^{N,k} + \delta_{\min}^{N,k})}{2}. \end{cases}$$

If $k = N$, $P_{322}^{N,N}$ is given by

$$\begin{aligned}
P_{322}^{N,N} &= \exp\left(-\frac{(\varpi + \theta_N)d_A^\alpha}{\lambda_A}\right) \times \\
&\quad \left[\exp\left(-\frac{(\varpi + \theta_N)d_B^\alpha}{\lambda_B}\right) - \exp\left(-\frac{\delta^{N,N}}{\lambda_B}\right) \right], \quad (28)
\end{aligned}$$

where $\delta^{N,N} = \max\left(\frac{\gamma_{\text{th}} d_B^\alpha}{2P_m X}, (\theta_N + \varpi)d_B^\alpha\right)$.

Case 3: When the energy harvester for P_{RF}^B works in the j -th linear region with $j \in \{1, \dots, N-1\}$, we have $(\varpi + \theta_j)d_B^\alpha \leq |h_B|^2 \leq (\varpi + \theta_{j+1})d_B^\alpha$.

(1) For the case $P_{\text{RF}}^A < P_{\text{th}}^1$, we have $k = 0$. Based on Eq. (18), there are two cases for $P_{322}^{j,0}$.

If $\Delta_{j,0} = (Y_{j,0}^{A3})^2 - 4Y^{A1}Y_{j,0}^{A2} < 0$, there is no $|h_B|^2$ that satisfies $Y_{j,0}^{A2}|h_B|^4 + Y_{j,0}^{A3}|h_B|^2 + Y^{A1} > 0$ and $P_{322}^{j,0} = 0$ always holds.

If $\Delta_{j,0} \geq 0$, there are two solutions to the equation $Y_{j,0}^{A2}|h_B|^4 + Y_{j,0}^{A3}|h_B|^2 + Y^{A1} = 0$, which are

$$\begin{cases} x_{j,0}^{B1} = \min\left(\frac{-Y_{j,0}^{A3} - \sqrt{\Delta_{j,0}}}{2Y_{j,0}^{A2}}, \frac{-Y_{j,0}^{A3} + \sqrt{\Delta_{j,0}}}{2Y_{j,0}^{A2}}\right), \\ x_{j,0}^{B2} = \max\left(\frac{-Y_{j,0}^{A3} - \sqrt{\Delta_{j,0}}}{2Y_{j,0}^{A2}}, \frac{-Y_{j,0}^{A3} + \sqrt{\Delta_{j,0}}}{2Y_{j,0}^{A2}}\right). \end{cases}$$

Combining with the condition that $(\varpi + \theta_j)d_B^\alpha \leq |h_B|^2 \leq (\varpi + \theta_{j+1})d_B^\alpha$, $P_{322}^{j,0}$ is given by

$$\begin{aligned}
P_{322}^{j,0} &= \mathbb{P}\left(\varpi d_A^\alpha \leq |h_A|^2 < (\theta_1 + \varpi)d_A^\alpha, \delta_{\min}^{j,0} \leq |h_B|^2 \leq \delta_{\max}^{j,0}\right) \\
&= \left(\exp\left(-\frac{\varpi d_A^\alpha}{\lambda_A}\right) - \exp\left(-\frac{(\theta_1 + \varpi)d_A^\alpha}{\lambda_A}\right) \right) \\
&\quad \times \left(\exp\left(-\frac{\delta_{\min}^{j,0}}{\lambda_B}\right) - \exp\left(-\frac{\delta_{\max}^{j,0}}{\lambda_B}\right) \right), \quad (29)
\end{aligned}$$

where

$$\begin{cases} \delta_{\min}^{j,0} = \min\left(\max\left((\varpi + \theta_j)d_B^\alpha, x_{j,0}^{B1}\right), (\varpi + \theta_{j+1})d_B^\alpha\right), \\ \delta_{\max}^{j,0} = \max\left(\min\left((\varpi + \theta_{j+1})d_B^\alpha, x_{j,0}^{B2}\right), \delta_{\min}^{j,0}\right). \end{cases}$$

(2) For the case $P_{\text{RF}}^A \in [P_{\text{th}}^j, P_{\text{th}}^{j+1}]$ with $j \in \{1, \dots, N-1\}$, $P_{322}^{j,k}$ with $j, k \in \{1, \dots, N-1\}$ is given by

$$\begin{aligned}
P_{322}^{j,k} &= \mathbb{P}\left((\varpi + \theta_k)d_A^\alpha \leq |h_A|^2 < \phi_{\max}^{j,k}, (\theta_j + \varpi)d_B^\alpha \leq |h_B|^2 < (\theta_{j+1} + \varpi)d_B^\alpha\right) \\
&= \left(\exp\left(-\frac{(\varpi + \theta_j)d_B^\alpha}{\lambda_B}\right) - \exp\left(-\frac{(\varpi + \theta_{j+1})d_B^\alpha}{\lambda_B}\right) \right) \times \\
&\quad \exp\left(-\frac{(\varpi + \theta_k)d_A^\alpha}{\lambda_A}\right) - \frac{1}{\lambda_B} \int_{(\varpi + \theta_j)d_B^\alpha}^{(\varpi + \theta_{j+1})d_B^\alpha} \exp\left(-\frac{\phi_{\max}^{j,k}(x)}{\lambda_A} - \frac{x}{\lambda_B}\right) dx, \quad (30)
\end{aligned}$$

where

$$\begin{aligned}
\phi_{\max}^{j,k}(x) &= \\
&\quad \max\left(\min\left(\frac{Y^{A1}}{a_k x} + \frac{Y_j^{A2}}{a_k} x + \frac{Y_j^{A3}}{a_k}, (\varpi + \theta_{k+1})d_A^\alpha\right), (\varpi + \theta_k)d_A^\alpha\right).
\end{aligned}$$

By using Gaussian-Chebyshev quadrature, the approximation of $P_{322}^{j,k}$ is given by

$$\begin{aligned}
P_{322}^{j,k} &\approx \left(\exp\left(-\frac{(\varpi + \theta_j)d_B^\alpha}{\lambda_B}\right) - \exp\left(-\frac{(\varpi + \theta_{j+1})d_B^\alpha}{\lambda_B}\right) \right) \\
&\quad \times \exp\left(-\frac{(\varpi + \theta_k)d_A^\alpha}{\lambda_A}\right) - \frac{\pi(\theta_{j+1} - \theta_j)d_B^\alpha}{2M\lambda_B} \\
&\quad \times \sum_{m=1}^M \sqrt{1 - \nu_m^2} \exp\left(-\frac{\phi_{\max}^{j,k}(\kappa_m^{j,k})}{\lambda_A} - \frac{\kappa_m^{j,k}}{\lambda_B}\right), \quad (31)
\end{aligned}$$

where $\kappa_m^{j,k} = \frac{(\theta_{j+1} - \theta_j)d_B^\alpha}{2} \nu_m + \frac{(2\varpi + \theta_j + \theta_{j+1})d_B^\alpha}{2}$.

(3) For the case $P_{\text{RF}}^A > P_{\text{th}}^N$, we have $k = N$ and $a_k = 0, b_k = P_m$. Based on Eq. (18), the value of $P_{322}^{j,N}$ depends on $\Delta_{j,N} = (Y_{j,N}^{A3})^2 - 4Y^{A1}Y_j^{A2}$. If $\Delta_{j,N} < 0$, similar to $P_{322}^{j,0}$, we have $P_{322}^{j,N} = 0$. If $\Delta_{j,N} \geq 0$, $P_{322}^{j,N}$ is given by

$$\begin{aligned}
P_{322}^{j,N} &= \mathbb{P}\left(|h_A|^2 > (\theta_N + \varpi)d_A^\alpha, \delta_{\min}^{j,N} \leq |h_B|^2 \leq \delta_{\max}^{j,N}\right) \\
&= \exp\left(-\frac{(\theta_N + \varpi)d_A^\alpha}{\lambda_A}\right) \left(\exp\left(-\frac{\delta_{\min}^{j,N}}{\lambda_B}\right) - \exp\left(-\frac{\delta_{\max}^{j,N}}{\lambda_B}\right) \right), \quad (32)
\end{aligned}$$

where

$$\begin{cases} \delta_{\min}^{j,N} = \min\left(\max\left((\varpi + \theta_j)d_B^\alpha, x_{j,N}^{B1}\right), (\varpi + \theta_{j+1})d_B^\alpha\right), \\ \delta_{\max}^{j,N} = \max\left(\min\left((\varpi + \theta_{j+1})d_B^\alpha, x_{j,N}^{B2}\right), \delta_{\min}^{j,N}\right), \\ x_{j,N}^{B1} = \min\left(\frac{-Y_{j,N}^{A3} - \sqrt{\Delta_{j,N}}}{2Y_j^{A2}}, \frac{-Y_{j,N}^{A3} + \sqrt{\Delta_{j,N}}}{2Y_j^{A2}}\right), \\ x_{j,N}^{B2} = \max\left(\frac{-Y_{j,N}^{A3} - \sqrt{\Delta_{j,N}}}{2Y_j^{A2}}, \frac{-Y_{j,N}^{A3} + \sqrt{\Delta_{j,N}}}{2Y_j^{A2}}\right). \end{cases}$$

Based on Eq. (16), the approximation of P_{out}^B can be obtained. Similarly, P_{out}^A can be obtained by the same way. Based on P_{out}^A and P_{out}^B , the capacity of the system C_{total} can be determined.

IV. SIMULATIONS

In this section, we validate the performance of the proposed scheme and the derived outage probability via 1×10^6 Monte-Carlo simulations. Unless otherwise specified, the simulation parameters are set as follows: $d_A = 15$ meters, $d_B = 10$ meters³, $\alpha = 3$, $\beta = \frac{1}{3}$

³The distances for source-relay and relay-destination links reflects the state of the art for sensor network applications. The typical single hop communications distance ranges from several meters to tens of meters.

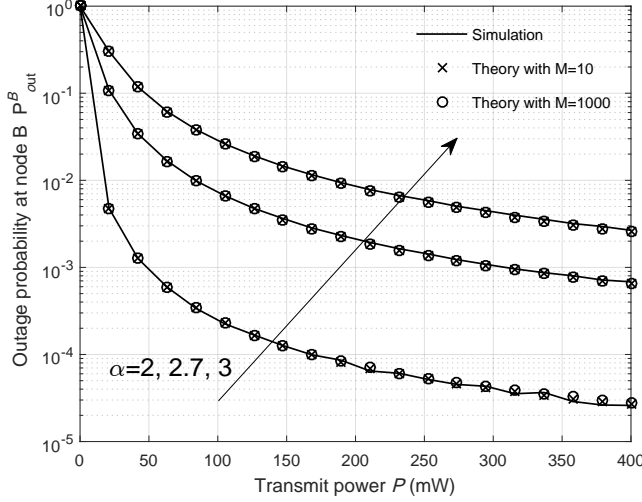


Fig. 2. Outage probability versus transmit power P .

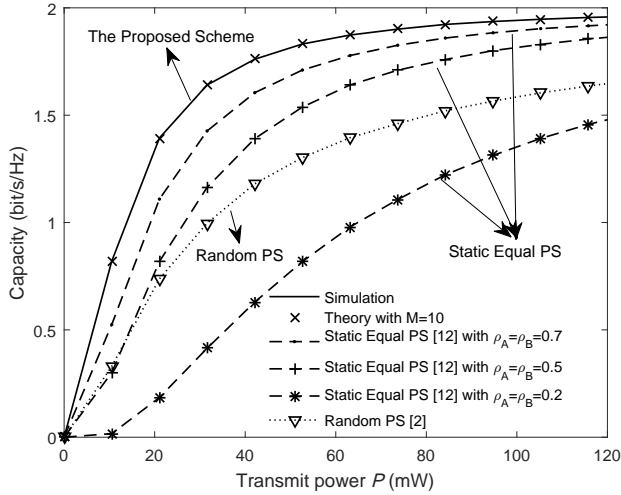


Fig. 3. Capacity versus transmit power P with $\alpha = 3$.

and $\sigma^2 = -90$ dBm. The transmission rate is assumed as $U = 3$ bit/s/Hz and the corresponding SNR threshold γ_{th} is $2^U - 1$. The transmit power of the source is set to be 10 mW. We employ the piecewise linear EH model with $N = 4$, where $P_{th} = [10, 57.68, 230.06, 100]$ uW, $\{a_k\}_1^3 = [0.3899, 0.6967, 0.1427]$, $\{b_k\}_1^3 = [-1.6613, -19.1737, 108.2778]$ uW and $P_m = 250$ uW. The accuracy of this model is verified by comparing it with the experimental data in [16].

Figure 2 plots the outage probability at B with the piecewise linear EH model achieved by the proposed scheme versus the transmit power with $\alpha = 2, 2.7$, and 3 , respectively. The theoretical results with different M are computed based on Eq. (14), Eq. (15), and Eq. (16). It can be observed that the theoretical results match perfectly with Monte Carlo simulation results, which verifies the accuracy of the theoretical results. Besides, it can also be seen that a small M (e.g. $M = 10$) is sufficient to provide an accurate P_{out}^B . Another observation is that the outage probability at node B converges to the error floors when the transmit power P keeps increasing, which

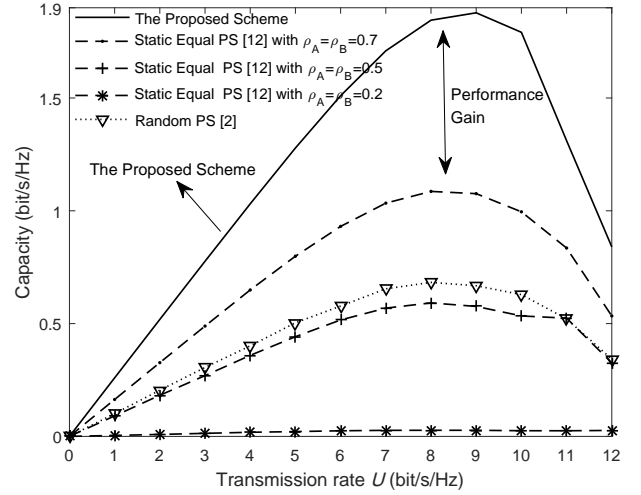


Fig. 4. Capacity versus transmission rate U with $\alpha = 3$.

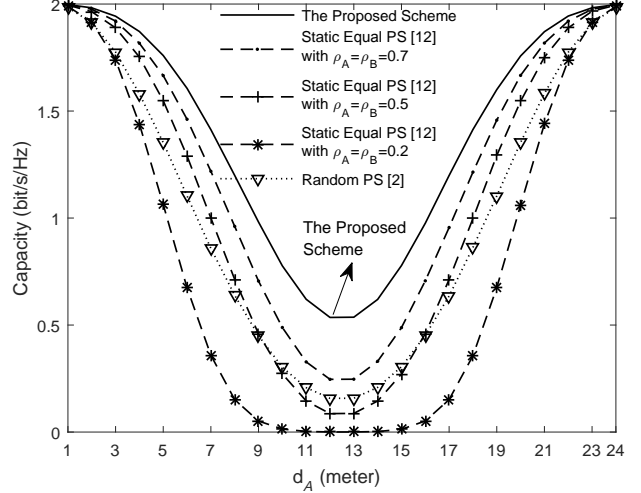


Fig. 5. Capacity versus the distance between A and R d_A with $\alpha = 3$.

is the main difference from the outage behaviors with the linear energy harvesting model. This is due to the fact that the harvested energy from A or B is constrained to P_m when P is large enough.

Figure 3 plots the capacity as a function of P with three PS schemes: the proposed scheme, the existing static equal scheme in [12], and the random PS scheme in [2]. For the random PS scheme, the PS ratio follows a uniform distribution over the closed interval $[0, 1]$. It can be observed that the capacity increases with the increase of P and converges to the maximum value when P is large enough, which perfectly matches the results in Fig. 2. Another observation is that the proposed scheme has a higher capacity than the existing schemes in [2] and [12]. The reason is that the proposed scheme can provide more flexibility and effectively utilize the instantaneous CSI.

Figure 4 plots the capacity for three PS schemes versus the transmission rate U . It can be seen that the capacity increases first, reaches the peak value, and then decreases. This is because that the outage probability at A or B goes up with

the increase of U and the influence of the outage probability becomes the dominant factor to the capacity when U is large enough. As shown in this figure, we can also see that the proposed scheme can provide a significant performance gain over the existing schemes. Fig. 5 compares the capacity of various PS schemes as a function of d_A . It is assumed that $d_A + d_B = 25$. Given a fixed d_A , d_B can be computed as $25 - d_A$. It can be observed that with the increase of d_A , the capacity decreases, reaches the minimum value and then increases. This is because that the total harvested energy is higher when the relay is closer to either of the nodes. Besides, we can see that the proposed scheme is superior to the existing schemes in terms of capacity.

V. CONCLUSIONS

In this paper, we have proposed a dynamic heterogeneous PS scheme to maximize the capacity of SWIPT based three-step DF TWRNs with a non-linear EH model. Specifically, by considering the heterogeneous instantaneous channel gains between the destination nodes and the relay, we have derived the closed-form expression of the optimal PS ratio for each link. Based on the optimal PS ratios, we have derived an analytical expression for the optimal outage probability under the non-linear EH model. Simulation results have verified the correctness of the derived outage probability and shown that the proposed PS scheme can achieve a higher capacity compared with the existing schemes.

ACKNOWLEDGMENTS

This work was supported in part by the National Natural Science Foundation of China (Nos. 61671347, 61771368 and 61701364), Young Elite Scientists Sponsorship Program By CAST (2016QNR001), the Fundamental Research Funds for the Central Universities, the National Natural Science Foundation of Shaanxi Province (2018JM6019) and the 111 Project of China (B08038). The work of Prof. R. Q. Hu was supported by the US National Science Foundations grants under the grants NeTS-1423348 and the EARS-1547312.

REFERENCES

- [1] W. Guo, S. Zhou, Y. Chen, S. Wang, X. Chu, and Z. Niu, "Simultaneous information and energy flow for IoT relay systems with crowd harvesting," *IEEE Commun. Mag.*, vol. 54, no. 11, pp. 143–149, November 2016.
- [2] H. Lee, C. Song, S. H. Choi, and I. Lee, "Outage probability analysis and power splitter designs for SWIPT relaying systems with direct link," *IEEE Commun. Lett.*, vol. 21, no. 3, pp. 648–651, March 2017.
- [3] Z. Chu, F. Zhou, Z. Zhu, R. Q. Hu *et al.*, "Wireless powered sensor networks for Internet of Things: Maximum throughput and optimal power allocation," *IEEE Internet Things J.*, vol. 5, no. 1, pp. 310–321, Feb 2018.
- [4] H. Sun, Q. Wang, S. Ahmed, and R. Q. Hu, "Non-orthogonal multiple access in a mmwave based IoT wireless system with SWIPT," in *2017 IEEE 85th VTC Spring*, June 2017, pp. 1–5.
- [5] L. Shi, L. Zhao, K. Liang, and H. H. Chen, "Wireless energy transfer enabled D2D in underlying cellular networks," *IEEE Trans. Veh. Technol.*, vol. 67, no. 2, pp. 1845–1849, Feb 2018.
- [6] Z. Ding, I. Krikidis, B. Sharif, and H. V. Poor, "Wireless information and power transfer in cooperative networks with spatially random relays," *IEEE Trans. Wireless Commun.*, vol. 13, no. 8, pp. 4440–4453, Aug 2014.

- [7] A. Alsharoa, H. Ghazzai, A. E. Kamal, and A. Kadri, "Wireless RF-based energy harvesting for two-way relaying systems," in *Proc. IEEE WCNC*, April 2016, pp. 1–6.
- [8] T. P. Do, I. Song, and Y. H. Kim, "Simultaneous wireless transfer of power and information in a decode-and-forward two-way relaying network," *IEEE Trans. Wireless Commun.*, vol. 16, no. 3, pp. 1579–1592, March 2017.
- [9] Y. Liu, L. Wang, M. ElKashlan, T. Q. Duong, and A. Nallanathan, "Two-way relaying networks with wireless power transfer: Policies design and throughput analysis," in *Proc. GLOBECOM*, Dec 2014, pp. 4030–4035.
- [10] S. T. Shah, K. W. Choi, S. F. Hasan, and M. Y. Chung, "Energy harvesting and information processing in two-way multiplicative relay networks," *Electron. Lett.*, vol. 52, no. 9, pp. 751–753, 2016.
- [11] Z. Wang, Y. Li, Y. Ye, and H. Zhang, "Dynamic power splitting for three-step two-way multiplicative AF relay networks," in *Proc. IEEE VTC-Fall*, Sept 2017, pp. 1–5.
- [12] N. T. P. Van, S. F. Hasan, X. Gui, S. Mukhopadhyay, and H. Tran, "Three-step two-way decode and forward relay with energy harvesting," *IEEE Commun. Lett.*, vol. 21, no. 4, pp. 857–860, April 2017.
- [13] G. Lu, L. Shi, and Y. Ye, "Maximum throughput of TS/PS scheme in an AF relaying network with non-linear energy harvester," *IEEE Access*, vol. 6, pp. 26 617–26 625, 2018.
- [14] Y. Ye, Y. Li, F. Zhou, N. Al-Dhahir, and H. Zhang, "Power splitting-based SWIPT with dual-hop DF relaying in the presence of a direct link," *IEEE Syst. J.*, pp. 1–5, 2018.
- [15] E. Boshkovska, D. W. K. Ng, N. Zlatanov, and R. Schober, "Practical non-linear energy harvesting model and resource allocation for SWIPT systems," *IEEE Commun. Lett.*, vol. 19, no. 12, pp. 2082–2085, Dec 2015.
- [16] T. Le, K. Mayaram, and T. Fiez, "Efficient far-field radio frequency energy harvesting for passively powered sensor networks," *IEEE J. Solid State Circuits*, vol. 43, no. 5, pp. 1287–1302, May 2008.
- [17] J. Guo and X. Zhu, "An improved analytical model for RF-DC conversion efficiency in microwave rectifiers," in *Proc. IEEE MTT S Int. Microwave Symp. Dig.*, June 2012, pp. 1–3.
- [18] X. Yue, Y. Liu, S. Kang, A. Nallanathan, and Y. Chen, "Modeling and analysis of two-way relay non-orthogonal multiple access systems," *IEEE Trans. Commun.*, vol. PP, no. 99, pp. 1–1, 2018.